JACS
JOURNAL OF THE AMERICAN CHEMICAL SOCIETY
Communication
pubs.acs.org/JACS

Naphthodithiophene–Naphthobisthiadiazole Copolymers for Solar Cells: Alkylation Drives the Polymer Backbone Flat and Promotes Efficiency

Itaru Osaka,*[,†,‡,∥] Takeshi Kakara,[†] Noriko Takemura,[†] Tomoyuki Koganezawa,[§] and Kazuo Takimiya*[,†,∥]

[†]Department of Applied Chemistry, Graduate School of Engineering, Hiroshima University, 1-4-1 Kagamiyama, Higashi-Hiroshima, Hiroshima 739-8527, Japan

[‡]Precursory Research for Embryonic Science and Technology, Japan Science and Technology Agency, Chiyoda-ku, Tokyo 102-0075, Japan

[§]Japan Synchrotron Radiation Research Institute, 1-1-1, Kouto, Sayo-cho, Sayo-gun, Hyogo 679-5198, Japan

[∥]Emergent Molecular Function Research Group, RIKEN Center for Emergent Matter Science (CEMS), Wako, Saitama 351-0198, Japan

Supporting Information

ABSTRACT: We show that rational functionalization of the naphthodithiophene core in copolymers based on naphthodithiophene and naphthobisthiadiazole improves the solubility without an alteration of the electronic structure. Surprisingly, the introduction of linear alkyl chains brings about a drastic change in polymer orientation into the face-on motif, which is beneficial for the charge transport in solar cells. As a result, the present polymers exhibit high power conversion efficiencies of up to ∼8.2% in conventional single-junction solar cells.

An enormous number of semiconducting polymers have been developed as p-type (electron-donor) materials for bulk heterojunction (BHJ) solar cells.[1] As a result of dramatic advances in molecular design and device architecture, the power conversion efficiency (PCE) of polymer-based BHJ solar cells has shown rapid improvement in the past few years.[2] However, PCEs of polymer-based conventional single-junction BHJ cells are typically in the range of 6–7%.[3] Although PCEs exceeding 8% were recently achieved,[2a,4] such high values are still limited, and therefore, the development of high-performance semiconducting polymers is highly awaited.

Key to the development of semiconducting polymers is the introduction of π cores that would ensure strong intermolecular interactions[5] and side chains with appropriate length, topology, and distribution,[2a,6] which would determine the crystallinity and orientation of the polymers in thin films and in turn the charge separation and charge transport properties. We recently reported that PNNT-DT, a copolymer comprising naphtho[1,2-*b*:5,6-*b*′]dithiophene (NDT3)[7] and naphtho[1,2-*c*:5,6-*c*′]bis[1,2,5]thiadiazole (NTz)[8] as the donor and acceptor units, respectively (Figure 1), exhibits good photovoltaic properties with a PCE of 4.9%.[9] However, a drawback of PNNT-DT is its low solubility, which severely hinders its processability. This is apparently attributed to the incorporation of highly π-extended four-ring-fused heteroaromatics. Here we demonstrate that upon the simple introduction of alkyl groups at the 5,10-positions of the NDT3 unit, the polymers show a substantial improvement of solubility as well as a change in the orientational order without an alteration of the energy levels, resulting in quite impressive PCEs in excess of 8% in a conventional single-junction solar cell.

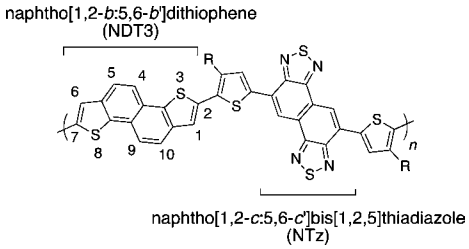

Figure 1. Structure of PNNT-DT (R = 2-decyltetradecyl).

Possible alkyl-substitution positions on the NDT3 core are the 1,6-positions (i.e., the β-positions of the thiophene rings) and the 4,9- and 5,10-positions (i.e., the inner and outer carbons, respectively, of the naphthalene substructure) (Figure 1). Alkyl substitution at the 1,6-positions yields a "head-to-head" arrangement between the alkylated NDT3 and alkylthiophene moieties, which reduces the backbone coplanarity and thus the intermolecular π–π interactions. Alkyl substitution at the 4,9- or 5,10-positions, on the other hand, does not sterically interfere with the other alkyl groups on the neighboring thiophene rings, preserving the coplanar backbone. In fact, the introduction of 4,9-dialkoxy-NDT3 in both oligomeric[10] and polymeric semiconductors[11] gave coplanar structures and promising performance in BHJ solar cells. However, the 4,9-positions allow the introduction of only alkoxy groups according to the reported synthetic methodology.[10] The strong electron-donating nature of the alkoxy group could raise the HOMO level (E_H) of the corresponding polymers relative to the polymers with naked or alkylated cores,[12] which would give rise to the low open-circuit voltage (V_{OC}).[13] In the meantime, we recently developed a method-

Received: April 24, 2013
Published: June 5, 2013

   dx.doi.org/10.1021/ja404064m | J. Am. Chem. Soc. 2013, 135, 8834–8837

Scheme 1. Synthesis of Semiconducting Polymers Comprising Alkylated NDT3 and NTz

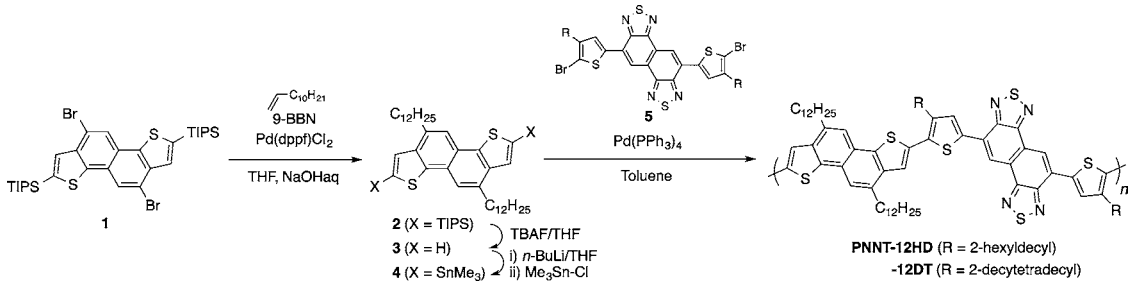

ology for functionalization at the 5,10-positions that allows us to introduce various functional moieties, including alkyl groups with a weaker electron-donating nature than alkoxy groups.[12]

Alkylation at the 5,10-positions of NDT3 was accomplished by means of a palladium-catalyzed cross-coupling reaction involving 5,10-dibromo-2,7-bis(triisopropylsilyl)-NDT3 (**1**), 9-borabicyclo[3.3.1]nonane (9-BBN), and dodecene (Scheme 1).[12] After removal of the TIPS groups to afford **3**, the 2,7-positions were easily stannylated to give comonomer **4**, which was then copolymerized with NTz-based comonomer **5** to yield PNNT-12HD and -12DT. The molecular weights and polydispersity indexes are M_n = 36.0 kDa (M_w = 88.9 kDa) and PDI = 2.5 for PNNT-12HD and M_n = 46.1 kDa (M_w = 139 kDa) and PDI = 3.0 for PNNT-12DT. The solubility of the polymer was greatly improved by the introduction of the alkyl chain. Whereas PNNT-DT is soluble only in hot chlorobenzene (CB) or *o*-dichlorobenzene (DCB), the newly synthesized polymers are soluble in chloroform, CB, and DCB at room temperature to 40 °C.

The E_H values for PNNT-12HD and -12DT were determined by photoelectron spectroscopy to be −5.22 eV, which is almost identical to that of PNNT-DT (−5.25 eV). This implies that the inductive effect of the alkyl groups at the 5,10-positions of the NDT3 core is small. This may partially be understood by the fact that the HOMO coefficient is not located at the 5,10-positions of the NDT3 core (Figure S1 in the Supporting Information). This insensitivity is particularly important because, again, a rise in E_H can cause a decrease in V_{OC}. Figure 2 shows the absorption spectra of PNNT-12HD and -DT. In both solution and films, the polymers showed similar spectra with absorption maxima at 660−670 nm. The absorption onsets in the film were found to be at 750−760 nm, corresponding to optical band gaps of 1.64−1.69 eV, indicating that the electronic structure is unchanged by the introduction of the alkyl groups.

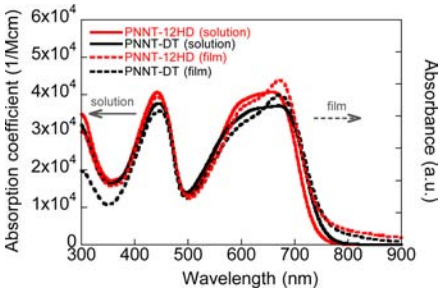

Figure 2. UV−vis absorption spectra of PNNT-12 and PNNT-DT in solution and films.

Next, the charge transport properties of the polymers were investigated using field-effect transistors. The hole mobilities (μ_{FET}) of PNNT-12HD and -12DT were found to be 0.01−0.1 $cm^2\ V^{-1}\ s^{-1}$, which are lower than that of PNNT-DT (~0.5 $cm^2\ V^{-1}\ s^{-1}$) (Figure S6 and Table 1). On the other hand, the charge carrier mobilities obtained from the space-charge-limited current model using hole-only devices (μ_{SCLC}) were ~10^{-3} $cm^2\ V^{-1}\ s^{-1}$ for both PNNT-12HD and -12DT in polymer-only and polymer/[6,6]-phenyl C_{61} butyric acid methyl ester ($PC_{61}BM$) blend films, whereas those of PNNT-DT were 1 order of magnitude lower (~10^{-4} $cm^2\ V^{-1}\ s^{-1}$) (Figure S7 and Table 1). Thus, charge transport in the in-plane direction was reduced by alkylation, but charge transport in the out-of-plane direction was enhanced.

The photovoltaic properties were investigated using a conventional BHJ cell (ITO/PEDOT:PSS/polymer:PCBM/LiF/Al). Note that no solvent additives were used at the time of spin-coating and no postdeposition treatments, such as thermal and/or solvent annealing, were carried out. Figure 3a shows the current density−voltage (J−V) curves for the PNNT/$PC_{61}BM$-based cells. The optimum polymer:$PC_{61}BM$ (p:n) weight ratios were 1:2 for PNNT-12HD but 1:1 for PNNDT-12DT and -DT. In the PNNT-12HD and -12DT cells with an active-layer thickness of 170−180 nm, the short-circuit current densities (J_{SC}) were 10.3 and 7.3 mA cm^{-2}, respectively, which are lower than that for the PNNT-DT cell with a similar thickness (12.3 mA cm^{-2}) (Table 2). Meanwhile, the V_{OC}'s of 0.84−0.86 V obtained for the cells with the present polymers are comparable to or even larger than those with PNNT-DT, consistent with the almost identical E_H. A striking feature of the cells using PNNT-12HD and -12DT is the high fill factor (FF) of >0.65 in comparison with that of cells using PNNT-DT (0.54); this is likely due to the efficient charge transport, as discussed above. As a result, the cells with PNNT-12HD and -12DT exhibited PCEs of 5.9% and 4.1%, respectively. The lower PCE for PNNT-12DT cells than for PNNT-12HD cells can be attributed to the nonideal morphology with large grains, as seen in the atomic force microscopy images (Figure S10).

More interestingly, the PCEs of the PNNT-12HD-based cells improved when thicker active layers were used (Figure 3c,d and Table 2). J_{SC} increased to 14.7 mA cm^{-2} as the active-layer thickness increased, although it seemed to saturate above 300 nm. It should be noted that the FF remained relatively high (i.e., >0.6) even when the thickness exceeded 300 nm, which has been seen in only a few polymers.[14] As a result, the PCE reached 7.5% for the cells that used $PC_{61}BM$ with an active-layer thickness of 290 nm. Furthermore, when $PC_{71}BM$ was used as the n-type material, the PNNT-12HD cells with a p:n ratio of 1:2 and a thickness of 300 nm exhibited a quite high PCE of 8.2% (J_{SC} = 15.6 mA cm^{-2}, V_{OC} = 0.82 V, FF = 0.64).

dx.doi.org/10.1021/ja404064m | J. Am. Chem. Soc. 2013, 135, 8834−8837

Table 1. Properties of PNNTs

side chain	M_n/M_w (kDa)[a]	E_H (eV)[b]	λ_{max} (nm)[c] solution	λ_{max} (nm)[c] film	E_g (eV)[d]	μ_{FET}[e] ($cm^2\ V^{-1}\ s^{-1}$)	μ_{SCLC}[f] ($cm^2\ V^{-1}\ s^{-1}$) polymer-only	μ_{SCLC}[f] ($cm^2\ V^{-1}\ s^{-1}$) blend
12HD	36.0/88.9	5.22	441, 657	442, 672	1.68	0.1	1.7×10^{-3}	3.0×10^{-3}
12DT	46.1/139	5.22	441, 656	443, 672	1.69	0.01	1.3×10^{-3}	2.0×10^{-3}
DT	31.0/310	5.25	445, 670	447, 672	1.64	0.5[g]	1.0×10^{-4}	1.4×10^{-4}

[a]Determined by GPC (DCB, 140 °C). [b]HOMO levels evaluated by photoelectron spectroscopy in air. [c]Absorption maxima in CB solution and thin films. [d]Optical band gaps determined from the absorption onsets in the films. [e]Hole mobilities evaluated with OFETs. [f]Hole mobilities evaluated with hole-only devices. [g]From ref 9.

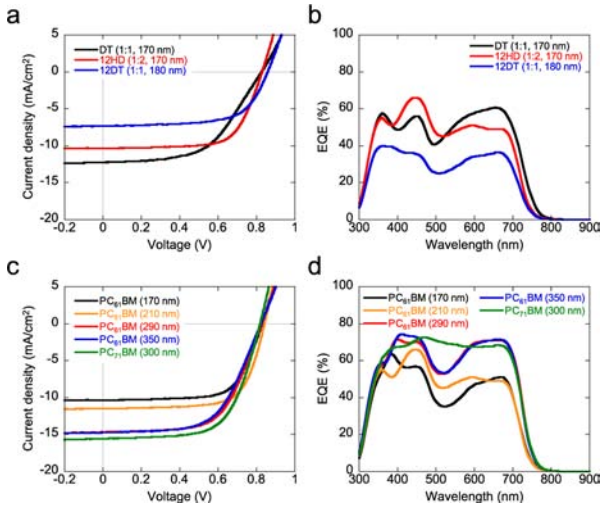

Figure 3. (a) $J-V$ curves and (b) EQE spectra of the polymer/$PC_{61}BM$-based cells with active-layer thicknesses of 170−180 nm. The p:n ratios are shown in the legend. (c) $J-V$ curves and (d) EQE spectra of PNNT-12HD-based cells (p:n = 1:2) with different active-layer thicknesses. The thicknesses are shown in the legend.

To correlate these performances, the ordering structure of the polymers was confirmed by two-dimensional grazing-incidence X-ray diffraction (2D-GIXD). As previously reported, PNNT-DT was oriented in an edge-on manner in the polymer-only film, as the diffractions corresponding to the lamellar structure and the π-stacking predominantly appeared along the q_z axis (q = 0.30 $Å^{-1}$) and the q_{xy} axis (q = 1.83 $Å^{-1}$), respectively (Figure 4a).[9] The lamellar d spacing (d_l) and π-stacking distance (d_π) were 21.1 and 3.43 Å, respectively, for PNNT-DT. We note that in sharp contrast, PNNT-12HD (Figure 4b) and -12DT (Figure S4) preferentially adopted the face-on orientation, as the π-stacking diffraction appeared along the q_z axis. The d_l value for PNNT-12DT was 28.1 Å, which is significantly larger than that for PNNT-DT, implying that the degree of side-chain interdigitation was smaller for PNNT-12DT and PNNT-12HD than for PNNT-DT. The d_π values for

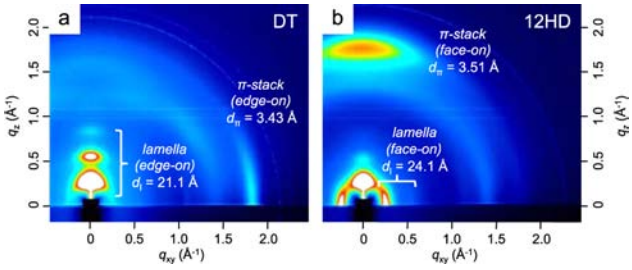

Figure 4. 2D-GIXD images of as-spun thin films of (a) PNNT-DT and (b) PNNT-12HD.

PNNT-12HD and -12DT (3.51−3.55 Å) were slightly larger than that for PNNT-DT. This face-on orientation in the present polymers came as a pleasant surprise for us, because (i) the PNNT backbone apparently prefers the edge-on orientation, as shown by the 2D-GIXD results for PNNT-DT, and (ii) in general, the introduction of linear alkyl groups triggers the edge-on orientation,[15] although it might depend on the backbone shape.[16] We speculated that the weakened intermolecular interactions, as evidenced by the larger values of d_l and d_π, which might originate in the increased side-chain density,[17] largely contributed to the drastically changed polymer orientation. Nevertheless, the crystalline π-stacking structure was still preserved in PNNT-12HD and -12DT. It should also be noted that when PNNT-12HD and -12DT were blended with $PC_{61}BM$, both d_π and d_l were unchanged, indicating that the polymer ordering was mostly preserved. The face-on orientation and the crystalline π-stacking of PNNT-12HD and -12DT are consistent with the low in-plane mobility and the high out-of-plane mobility compared with PNNT-DT, and again, this would presumably contribute to the greatly improved FF of the BHJ cells, even with the thicker active layer. It is interesting to note that even though PNNT-DT also formed the face-on orientation in the presence of $PC_{61}BM$ (Figure S9),[9] the μ_{SCLC} and FF were significantly lower than for the present polymers. This suggests that control of the primary ordering structure is quite important to achieve high efficiencies.

Table 2. Photovoltaic Properties of BHJ Solar Cells Based on PNNTs

side chain	n-type material	p:n[a]	thickness (nm)[b]	J_{SC} (mA cm^{-2})	V_{OC} (V)	FF	PCE_{max} [PCE_{ave}] (%)[c]
12HD	$PC_{61}BM$	1:2	170	10.3	0.83	0.68	5.9 [5.5]
			210	11.5	0.84	0.69	6.7 [6.5]
			290	14.7	0.83	0.61	7.5 [7.3]
			350	14.7	0.83	0.60	7.3 [7.0]
	$PC_{71}BM$	1:2	300	15.6	0.82	0.64	8.2 [8.0]
12DT	$PC_{61}BM$	1:1	180	7.3	0.86	0.65	4.1 [4.0]
DT	$PC_{61}BM$	1:1	170	12.3	0.83	0.54	5.5 [5.2]

[a]Polymer (p) to PCBM (n) weight ratio. [b]Active-layer thickness. [c]PCE_{max} = maximum PCE, PCE_{ave} = average PCE.

dx.doi.org/10.1021/ja404064m | J. Am. Chem. Soc. 2013, 135, 8834−8837

In conclusion, we have demonstrated that the careful choice of the functionalization position and the functional group on the NDT3 unit in the corresponding copolymer with NTz can greatly improve the solubility without altering the electronic properties. A substantial change in the polymer orientation from edge-on to face-on was accompanied by the alkylation, facilitating the out-of-plane charge transport. BHJ cells based on the present copolymers exhibited PCEs as high as 8.2% using only an as-spun active layer with a thickness of 300 nm. These results indicate that this polymer platform is of particular interest in developing further high-performance polymers.

■ ASSOCIATED CONTENT

Supporting Information

Synthesis, characterization, computation, and thin-film analyses of the materials. This material is available free of charge via the Internet at http://pubs.acs.org.

■ AUTHOR INFORMATION

Corresponding Author

itaru.osaka@riken.jp; takimiya@riken.jp

Notes

The authors declare no competing financial interest.

■ ACKNOWLEDGMENTS

This work was supported by Grants-in-Aid for Scientific Research (24685030 and 23245041) from MEXT, the Strategic Promotion of Innovative Research and Development from JST, and NEDO. The 2D-GIXD experiments were performed at BL19B2 of SPring-8 with the approval of the Japan Synchrotron Radiation Research Institute (JASRI) (Proposal 2012B1728). We thank Prof. D. Yokoyama (Yamagata University) for useful discussion on the hole-only device measurement.

■ REFERENCES

(1) (a) Facchetti, A. *Chem. Mater.* **2011**, *23*, 733. (b) Beaujuge, P. M.; Fréchet, J. M. J. *J. Am. Chem. Soc.* **2011**, *133*, 20009. (c) Boudreault, P.-L. T.; Najari, A.; Leclerc, M. *Chem. Mater.* **2011**, *23*, 456.

(2) (a) Cabanetos, C.; Labban, A. D.; Bartelt, J. A.; Douglas, J. D.; Mateker, W. R.; Fréchet, J. M. J.; McGehee, M. D.; Beaujuge, P. M. *J. Am. Chem. Soc.* **2013**, *135*, 4656. (b) You, J.; Dou, L.; Yoshimura, K.; Kato, T.; Ohya, K.; Moriarty, T.; Emery, K.; Chen, C.-C.; Gao, J.; Li, G.; Yang, Y. *Nat. Commun.* **2013**, *4*, 1446.

(3) (a) Liang, Y.; Yu, L. *Acc. Chem. Res.* **2010**, *43*, 1227. (b) Chen, J.; Cao, Y. *Acc. Chem. Res.* **2009**, *42*, 1709.

(4) (a) Chen, H.-C.; Chen, Y.-H.; Liu, C.-C.; Chien, Y.-C.; Chou, S.-W.; Chou, P.-T. *Chem. Mater.* **2012**, *24*, 4766. (b) Small, C. E.; Tsang, S.-W.; Chen, S.; Baek, S.; Amb, C. M.; Subbiah, J.; Reynolds, J. R.; So, F. *Adv. Energy. Mater.* **2013**, DOI: 10.1002/aenm.201201114.

(5) (a) Mühlbacher, D.; Scharber, M.; Morana, M.; Zhu, Z.; Waller, D.; Gaudiana, R.; Brabec, C. *Adv. Mater.* **2006**, *18*, 2884. (b) Hou, J.; Chen, H.-Y.; Zhang, S.; Li, G.; Yang, Y. *J. Am. Chem. Soc.* **2008**, *130*, 16144. (c) Liang, Y.; Wu, Y.; Feng, D.; Tsai, S.-T.; Son, H.-J.; Li, G.; Yu, L. *J. Am. Chem. Soc.* **2009**, *131*, 56.

(6) (a) Szarko, J. M.; Guo, J.; Liang, Y.; Lee, B.; Rolczynski, B. S.; Strzalka, J.; Xu, T.; Loser, S.; Marks, T. J.; Yu, L.; Chen, L. X. *Adv. Mater.* **2010**, *22*, 5468. (b) Yiu, A. T.; Beaujuge, P. M.; Lee, O. P.; Woo, C. H.; Toney, M. F.; Fréchet, J. M. J. *J. Am. Chem. Soc.* **2012**, *134*, 2180. (c) Yang, L.; Zhou, H.; You, W. *J. Phys. Chem. C* **2010**, *114*, 16793.

(7) (a) Shinamura, S.; Miyazaki, E.; Takimiya, K. *J. Org. Chem.* **2010**, *75*, 1228. (b) Shinamura, S.; Osaka, I.; Miyazaki, E.; Nakao, A.; Yamagishi, M.; Takeya, J.; Takimiya, K. *J. Am. Chem. Soc.* **2011**, *133*, 5024. (c) Osaka, I.; Abe, T.; Shinamura, S.; Miyazaki, E.; Takimiya, K. *J. Am. Chem. Soc.* **2010**, *132*, 5000. (d) Osaka, I.; Abe, T.; Shinamura, S.; Takimiya, K. *J. Am. Chem. Soc.* **2011**, *133*, 6852.

(8) (a) Wang, M.; Hu, X.; Liu, P.; Li, W.; Gong, X.; Huang, F.; Cao, Y. *J. Am. Chem. Soc.* **2011**, *133*, 9638. (b) Osaka, I.; Shimawaki, M.; Mori, H.; Doi, I.; Miyazaki, E.; Koganezawa, T.; Takimiya, K. *J. Am. Chem. Soc.* **2012**, *134*, 3498.

(9) Osaka, I.; Abe, T.; Shimawaki, M.; Koganezawa, T.; Takimiya, K. *ACS Macro Lett.* **2012**, *1*, 437.

(10) Loser, S.; Miyauchi, M.; Hennek, J. W.; Smith, J.; Huang, C.; Facchetti, A.; Marks, T. J. *Chem. Commun.* **2012**, *48*, 8511.

(11) (a) Shi, S.; Jiang, P.; Yu, S.; Wang, L.; Wang, X.; Wang, M.; Wang, H.; Li, Y.; Li, X. *J. Mater. Chem. A* **2013**, *1*, 1540. (b) Bathula, C.; Song, C. E.; Badgujar, S.; Hong, S.-J.; Park, S. Y.; Shin, W. S.; Lee, J.-C.; Cho, S.; Ahn, T.; Moon, S.-J.; Lee, S. K. *Polym. Chem.* **2013**, *4*, 2132.

(12) Shinamura, S.; Sugimoto, R.; Yanai, N.; Takemura, N.; Kashiki, T.; Osaka, I.; Miyazaki, E.; Takimiya, K. *Org. Lett.* **2012**, *14*, 4718.

(13) Liang, Y.; Feng, D.; Wu, Y.; Tsai, S.-T.; Li, G.; Ray, C.; Yu, L. *J. Am. Chem. Soc.* **2009**, *131*, 7792.

(14) (a) Peet, J.; Wen, L.; Byrne, P.; Rodman, S.; Forberich, K.; Shao, Y.; Drolet, N.; Gaudiana, R.; Dennler, G.; Waller, D. *Appl. Phys. Lett.* **2011**, *98*, No. 043301. (b) Price, S. C.; Stuart, A. C.; Yang, L.; Zhou, H.; You, W. *J. Am. Chem. Soc.* **2011**, *133*, 4625. (c) Li, W.; Hendriks, K. H.; Roelofs, W. S. C.; Kim, Y.; Wienk, M. M.; Janssen, R. A. J. *Adv. Mater.* **2013**, DOI: 10.1002/adma.201300017.

(15) (a) Osaka, I.; Zhang, R.; Liu, J.; Smilgies, D.-M.; Kowalewski, T.; McCullough, R. D. *Chem. Mater.* **2010**, *22*, 4191. (b) Subramaniyan, S.; Xin, H.; Kim, F. S.; Shoaee, S.; Durrant, J. R.; Jenekhe, S. A. *Adv. Energy Mater.* **2011**, *1*, 854.

(16) Guo, J. C.; Liang, Y. Y.; Szarko, J.; Lee, B.; Son, H. J.; Rolczynski, B. S.; Yu, L.; Chen, L. X. *J. Phys. Chem. B* **2010**, *114*, 742.

(17) Zhang, X.; Ritcher, L. J.; Delongchamp, D. M.; Kline, R. J.; Hammond, M. R.; McCulloch, I.; Heeney, M.; Ashraf, R. S.; Smith, J. N.; Anthopoulos, T. D.; Schroeder, B.; Geerts, Y. H.; Fischer, D. A.; Toney, M. F. *J. Am. Chem. Soc.* **2011**, *133*, 15073.